

DECENTRALIZED ADAPTIVE CONTROL OF A TWO DEGREE OF FREEDOM FLEXIBLE ARM

B. S. Yuan, W. J. Book, and J. D. Huggins
School of Mechanical Engineering
Georgia Institute of Technology
Atlanta, Georgia

ABSTRACT

A robust adaptive control is derived by signal-synthesis methods for a light, flexible two degree-of-freedom manipulator. The controller for each joint is decentralized, using measurements of one joint's position as well as one link's strain. The coupling to other dynamics is treated as a bounded uncertainty in the model. A stability proof has been developed and is outlined. Performance of the advanced controller is compared to a Linear Quadratic Regulator (LQR) and to an independent joint control. Both simulations and experiments are presented. The cases of payload variations are considered at this point.

I. INTRODUCTION

The industrial robotic arm has been designed for rigidity by implementing short link lengths and heavy steel construction in order to achieve positional accuracy and stability of the robot's movement. The resulting disadvantages include slow motion speed, low payload to weight ratio and high power consumption. To overcome these issues, a robotic arm with a light-weight structure poses an important solution for the designer of the next generation of robots. The main problem with light-weight structures is in the resulting flexible vibrations which are naturally excited as the arm is commanded to move or is disturbed. An effective control is one key to moving the flexible arm with high-speed motion and fast vibration settling time [1,2].

In order to demonstrate the control system of a flexible arm, a large flexible manipulator arm, designated RALF (Robotic Arm, Large and Flexible), is used in the experiment. The robotic system with the independent joint PD (Proportional-Derivative) controller, which is proven to be stable via the Lyapunov criterion, leads to the development of an advanced control algorithm using a decentralized scheme. In other words, each flexible link can be considered as a subsystem of the overall system. Under consideration of the uncertainty for interconnected terms of each subsystem, the dynamic system of the manipulator motion is illustrated to be bounded by the reference model, which is chosen to be stable. The possible magnitude of the uncertainty is presumed known, making the statistical information for a stochastic approach unnecessary [3]. Thus, the feedback systems are also insensitive to other uncertainties such as friction, measurement error, backlash and etc.

Certain matching conditions are assumed to guarantee that the uncertainty vector does not influence the dynamics more than the control input does [4]. The signal-synthesis adaptation approach used here results in a robust design that reduces the burden of on-line computation, while an auxiliary input with the update action should have faster convergence rate and smaller steady-state error.

Simulations and experiments are carried out to compare this controller to the independent joint PD controller and an LQR controller. The sensitivity of the control performance to variations in payload ranging from 0% to 40% of the arm structure is considered.

II. DYNAMIC MODELING AND INDEPENDENT JOINT CONTROLLER

To specify the robot controller, the dynamical equations of motion need to be developed for the system design [5]. A rigid arm will have one generalized coordinate per joint, but a flexible arm may have many. Transformations representing the joint coordinates and link deflection can be used to represent the position r_i of a point. The velocity can be related to the coordinate derivatives as [7]

$$\dot{r}_i = J_i \dot{X}_i, \quad (2.1)$$

where

\dot{r} is the velocity vector in the Cartesian coordinates,
 J_i is the $3 \times L$ matrix of Jacobian,
 \dot{X}_i represents the time derivative vector including i joints,
say, q_1, q_2, \dots, q_i , and L_i - i time dependent flexible coordinates.

The kinetic energy of the n -link flexible arm is then:

$$KE = \frac{1}{2} \sum_{i=1}^n \int_{link_i} \dot{r}_i^T \dot{r}_i dm \quad (2.2a)$$

$$= \frac{1}{2} \sum_{i=1}^n \dot{X}_i^T \left[\int_{link_i} J_i^T J_i dm \right] \dot{X}_i$$

$$= \frac{1}{2} \dot{X}_n^T M \dot{X}_n,$$

where

$$M = \sum_{i=1}^n \int_{link_i} \left[J_i^T J_i \right] dm. \quad (2.2b)$$

It is mentioned that the inertia matrix M , a function of position, is symmetric and positive definite. The kinetic energy of rigid robotic arms have the same structure as (2.2a)

Without the effect of gravity, the potential energy of the flexible arm which includes the elastic joint and strain energy is expressed as

$$PE = \frac{1}{2} \bar{X}^T K \bar{X}, \quad (2.3)$$

where

$\bar{X} = X - X_0$, X_0 is the unstretched coordinate at the "home" position.

K is the stiffness matrix, which has the corresponding value as described in Ref. [7].

By applying the Lagrangian formula, the equation of motion in the Matrix-Vector form is:

$$M \ddot{X} + H\dot{X} + K\bar{X} = Q, \quad (2.4)$$

where

Q is the generalized force, which acts on the joint q only.
 H represents nonlinear terms and $(M - 2H)$ is skew symmetric.

The similar form has also been found in the rigid arms without the stiffness term K .

Hence, a multi-link flexible arm with independent joint controllers will be stable. The case of a rigid-link manipulator has been illustrated by Asada and Slotine [5]. The frequency domain approach has been taken by Book [1] for flexible arms, and physically, the feedback system effectively equips each joint with an equivalent rotary spring and damper. The input torque then has the following form:

$$\tau_i = K_{pi} \bar{q}_i + K_{di} \dot{\bar{q}}_i, \quad (2.5)$$

where

K_{pi} and K_{di} are positive constants,
 $\bar{q}_i = q_i - q_{i0}$, q_{i0} is the reference path and assumed to be constant. $\dot{q}_i = \dot{q}_i$.

Because the torque acts only on each joint, the following equality exists

$$Q^T \dot{X} = \tau^T \dot{q}, \quad (2.6)$$

where

$$\tau^T = [\tau_1, \tau_2, \dots, \tau_n], \quad q^T = [q_1, q_2, \dots, q_n],$$

Choose a Lyapunov candidate V associated with the total energy of the feedback system:

$$V(\dot{X}, \bar{X}, q) = \frac{1}{2} \dot{X}^T M \dot{X} + \bar{X}^T K \bar{X} + \bar{q}^T K_p \bar{q}, \quad (2.7)$$

where

$$K_p = \text{diag} [K_{pi}]$$

Differentiating V with respect to time gives

$$\begin{aligned} \dot{V} &= \dot{q}^T K_p \bar{q} + \dot{X}^T M \dot{X} + \frac{1}{2} \dot{X}^T \dot{M} \dot{X} + \dot{X}^T K \bar{X} \\ &= \dot{q}^T K_p \bar{q} + \dot{X}^T (M + K\bar{X}) + \frac{1}{2} \dot{X}^T \dot{M} \dot{X} \end{aligned} \quad (2.8a)$$

By substituting (2.5), (2.6), (2.4) and the skew-symmetry of $(\dot{M} - 2H)$ into above,

$$\begin{aligned} \dot{V} &= \dot{q}^T K_p \bar{q} + \dot{X}^T (Q - H\dot{X}) + \frac{1}{2} \dot{X}^T \dot{M} \dot{X} \\ &= \dot{q}^T K_p \bar{q} + \dot{X}^T Q + \frac{1}{2} \dot{X}^T (\dot{M} - 2H) \dot{X} \\ &= \dot{q}^T K_p \bar{q} + \dot{q}^T \tau \\ &= -\dot{q}^T K_D \dot{q} \leq 0 \end{aligned}$$

where

$K_D = \text{diag}[k_{di}]$ is a positive matrix.

Therefore, the system with a local joint PD controller leads to the development of an advanced control algorithm using a decentralized scheme which is restrictive on information transfer from one group of sensors and actuators to others.

III. DECENTRALIZED ADAPTIVE CONTROL

Without loss of generality, the system of a two-degree-of-freedom flexible manipulator with the effect of gravity is considered from the control viewpoint; i.e., $n=2$. To combine with friction and other disturbances that are treated as uncertainties $R(X, \dot{X})$, the equations of motion are, then, rewritten as follows:

$$M(X)\ddot{X} + H(X, \dot{X})\dot{X} + K\bar{X} + G(X) + R(X, \dot{X}) = Q \quad (3.1)$$

The actuator dynamics is ignored.

Since the inertia matrix, $M(X)$, is square, symmetric and positive definite, one can always find a constant matrix β such that the elements of β corresponding to the coupling subsystem are zero and

$$\|\beta\| \geq \|M^{-1}(X) - \beta\| \quad (3.2)$$

where $\|\cdot\|$ is an induced norm.

Equation (3.1) can be rearranged as

$$\ddot{X} = -M^{-1}[H\dot{X} + K\bar{X} + G + R] + \beta Q + (M^{-1} - \beta)Q \quad (3.3)$$

With $i = 1, 2$, let $z_i = [x_i, \dot{x}_i]^T$ and equation (3.3) is divided into two equations for two subsystems,

$$\dot{z}_i = A_i z_i + b_i u_i + F_i(Z) + f_i(Z) u_i \quad (3.4)$$

where $u_i = \tau_i$ in (2.6); $f_i(Z)u_i$ = the coupling terms of $(M^{-1} - \beta)Q$ for subsystem i . A_i is a constant matrix which represents the linear time invariant part of $-M^{-1}K$,

$$A_i = \begin{bmatrix} 0 & I \\ a_{i1} & a_{i2} \end{bmatrix} \quad (3.5)$$

while $F_i(Z)$ represents the rest of $-M^{-1}K$ and the nonlinear terms of $-M^{-1}[H + R + G]$. b_i , then, becomes a vector form with zero elements on the upper half.

It is assumed that F_i and f_i are bounded and have the following properties:

$$F_i(Z) = b_i D_i(Z) \quad (3.6)$$

$$f_i(Z) = b_i E_i(Z)$$

where D_i and E_i have the corresponding dimensions; $\|E_i\| < 1$ from (3.2).

These conditions, called the matching conditions [8], guarantee that the uncertainty does not influence the dynamics more than the control input does [4]. The one degree-of-freedom system, has been illustrated by the previous works [9], and for the two degree-of-freedom flexible arm, each link is considered as a subsystem.

The objective of model reference adaptive control is to eliminate the state error between the plant and the reference model so that the behavior of the plant follows the model. Consider the reference model first,

$$\dot{z}_{mi} = A_{mi} z_{mi} + b_{mi} r_i \quad (3.7a)$$

where

$$z_{mi} = [x_{mi}, \dot{x}_{mi}]^T$$

r_i is the reference input,

and let

$$A_{mi} = A_i + b_i K_{zi} \quad (3.7b)$$

$$b_{mi} = b_i K_{bi}$$

where K_{zi} and K_{bi} are constant matrices with the corresponding dimensions.

Also, A_{mi} , which is a stable matrix, satisfies the Lyapunov equation,

$$A_{mi}^T P_i + P_i A_{mi} = -L_i \quad (3.7c)$$

where P_i and L_i are positive definite and symmetric matrices.

The signal-synthesis method [10] implemented here seeks to control the system by adjusting the input u_i which is as described in the following equation

$$u_i = K_{zi} z_i + K_{bi} r_i + \psi_i(e_i) \quad (3.8)$$

where $e_i = z_{mi} - z_i$ is referred to as the state error and the function ψ_i is the control input to compensate the system uncertainty. Thus, let ψ_i be

$$\psi_i = \begin{cases} \frac{b_i^T P_i e_i}{\|b_i^T P_i e_i\|} \rho_i(Z, e_i, r_i), & \text{when } \|b_i^T P_i e_i\| > \delta_i \\ \frac{b_i^T P_i e_i}{\delta_i} \rho_i(Z, e_i, r_i), & \text{when } \|b_i^T P_i e_i\| \leq \delta_i \end{cases} \quad (3.9)$$

where δ_i is a prescribed positive constant and ρ_i is a positive constant to be specified subsequently.

As a result, the error dynamics of the subsystem is derived from the difference between equation (3.4) and (3.7) along with (3.8) and (3.9):

$$\dot{e}_i = \dot{z}_{mi} - \dot{z}_i = A_{mi} e_i - b_i(\psi_i + \nu_i), \quad (3.10a)$$

where

$$\nu_i = D_i + E_i(K_{zi} + K_{bi} r_i + \psi_i) \quad (3.10b)$$

Given the boundedness of the state variable z_i and the reference input r_i , equation (3.10b) with (3.9) has the following inequality:

$$\|\nu_i\| \leq \rho_i(Z, \rho_i, r_i), \quad (3.11a)$$

where

$$\rho_i \triangleq \|D_i\| + \|E_i\|(\|K_{zi} z_i\| + \|K_{bi} r_i\| + \|\psi_i\|) \quad (3.11b)$$

This definition involving ρ_i on both sides of the equation is valid; i.e., (3.11) can be solved, since (3.2) is satisfied. Therefore, we have

$$\rho_i = (1 - \|E_i\|)^{-1} [\|D_i\| + \|E_i\|(\|K_{zi} z_i\| + \|K_{bi} r_i\|)] \quad (3.12)$$

To specify that the error dynamics (3.10) is uniformly bounded, the approach is also based on the Lyapunov criterion and similar to ref. [8]. Given a candidate

$$V_i = e_i^T P_i e_i, \quad (3.13a)$$

and there exists

$$\begin{aligned} \dot{V}_i &= \dot{e}_i^T P_i e_i - 2e_i^T P_i b_i(\psi_i + \nu_i) \\ &\leq e_i^T L_i e_i - 2[b_i^T P_i e_i][\psi_i - \frac{b_i^T P_i e_i}{\|b_i^T P_i e_i\|} \rho_i] \end{aligned} \quad (3.13)$$

Consequently, $\dot{V}_i \leq 0$

Furthermore, to improve the convergence rate of equation (3.10), an auxiliary input $w_i(t)$ is introduced and applied to the input u_i in (3.8) [7]. This input is apparently an integral action and

$$\dot{w}_i(t) = -\alpha_i w_i(t) + S_i^{-1} b_i^T P_i e_i, \quad (3.14)$$

where

$$\alpha_i \geq \frac{4 \delta_i \rho_i - \lambda_{\min}(L_i) \|\rho_i\|^2}{2 \lambda_{\min}(S_i) \|w_i\|^2}$$

$$S_i > 0$$

Note that λ_{\min} represents the minimum eigenvalue.

The error dynamics of the total system can be proven stable by summing the individual Lyapunov function (3.13) [7]. The block diagram of the decentralized adaptive control is shown in Figure 1.

IV. SIMULATIONS AND EXPERIMENTS

The following section will demonstrate the results obtained from the analytical works using RALF, which is in the Flexible Automation Laboratory at Georgia Tech. The arm is constructed of two ten foot links and two rotary joints. The second joint is actuated through a parallelogram mechanism by a hydraulic cylinder at the base [11]. A simple yet adequate dynamical model for RALF has been established, wherein the parallel link is described simply as a spring [7].

A MicroVax II running the VMS operating system is used to provide high speed calculation for real-time control and data-acquisition. The resolution of D/A and A/D is 12 bits/10 Volts, and the sampling time is 8 ms. For the initial measurement, the bandwidth of both hydraulic motors is above 45 Hz and the lowest frequencies of the RALF are 5.69 Hz and 9.12 Hz. The parallel link's lowest frequency is about 30 Hz, which cannot be controlled. A linear variable differential transformer (LVDT) is the position transducer mounted on the hydraulic piston rod, so that the noncollocation problem existing in the feedback control of flexible structures may be avoided. The link deflection is obtained by utilizing a strain gage mounted near the joint. One flexible mode is adopted for each link in this work.

The first joint position of 35° and the second joint position of 109° are set to be the "home" position for RALF. A linearized dynamical equation is used to derive the constant gains K_{zi} and K_{bi} in (3.7) and (3.8), while the payload is not considered at this moment [11]. K_{zi} ($i=1,2$) are:

$$K_{z1} = [-2.8E7 \ -1.35E4 \ -2.8E5 \ -1.14E3] , \quad (4.1)$$

$$K_{z2} = [-3.0E7 \ -1.01E4 \ -7.76E4 \ -2.68E2] ,$$

and $Kb_1 = 1$.

The gains associated with the joint positions and velocities turn out to be the independent joint controller in (2.5) as follows:

$$K_p = \begin{bmatrix} 2.8E7 & 0 \\ 0 & 3.0E7 \end{bmatrix} \quad (4.2)$$

$$K_D = \begin{bmatrix} 2.8E5 & 0 \\ 0 & 7.76E4 \end{bmatrix}$$

To get b_1 , equation (3.2) needs to be satisfied and β has the interconnecting elements of zero. Thus, b_1 and b_2 are:

$$b_1 = \begin{bmatrix} 0 \\ 0 \\ 0.002 \\ -0.259 \end{bmatrix} \quad (4.3)$$

$$b_2 = \begin{bmatrix} 0 \\ 0 \\ 0.0373 \\ -5.267 \end{bmatrix}$$

The values of ρ_i and δ_i are chosen as $3.0E5$ and 2.0 respectively. For the decentralized adaptive control, S_i^{-1} is $3.0E2$ and α_i is simply set to zero.

The distal ends of both the lower and the upper links are moved 24.3 inches in 1 second for joint point-to-point control. Figures 2a-d show the time responses of the feedback system without payload, and Figures 3a-d show results with a 30 lb payload. Note that the best tracking and fast oscillation-setting time of each link occurs with adaptation but that the link oscillations damped out more slowly for the joint PD control and LQR, when the system has the payload on the tip. However, all of the three controllers demonstrate the robustness with the variation of payload. When the controller is implemented in the experiment, the gains are scaled to match the physical capability of the system. Figures 4a,b show the time responses of the joints with the PD controller and with the decentralized adaptive controller without payload. The strain responses are demonstrated in Figures 4c-f. With payload, the response is as shown in Figures 5. It should be mentioned that the gravitational effect provides the partial reason for the steady-state error in the joint PD control.

The results from simulations are compared with the experiments to illustrate certain agreement. The fact that the simplified model, (the actuator dynamics ignored and one flexible mode used), implemented in the simulation may cause small deviation from the measured experimental data is, however, expected and acceptable from the engineering point of view.

V. CONCLUSION

A flexible arm with positive gains and negative feedback independently controlling each joint is shown theoretically and experimentally to be stable. The decentralized algorithm results have shown much improvement of the system responses. To achieve insensitivity to variations of the payload, the adaptive scheme of control is superior. The assumption of banded and small interconnecting action between subsystems is consequently appropriate.

ACKNOWLEDGEMENTS

This work was partially supported through NASA Grant NAG1-623 and the Computer Integrated Manufacturing Systems Program at the Georgia Institute of Technology.

REFERENCES

- [1] Book, W. J., "Model, design and control flexible manipulator arms," Ph.D. Thesis, Dept. of Mech. Engr. MIT, April 1974.
- [2] Cannon, R. M., Schmitz, E., "Initial experiments on the end-point control of a flexible one-link robot," *Int. J. of Robotics Research*, Fall 1984, pp. 62-75.
- [3] Chen, Y. H., "On the deterministic performance of uncertain dynamical systems," *Int. J. Control*, Vol.43, 1986, pp.521-525.
- [4] Gutman, S., "Uncertain dynamical systems - a Lyapunov Min-Max approach," *IEEE Trans. on Auto. Control*, June 1979.
- [5] Asada, H., Slotine, J. J., *Robot analysis and control*, John Wiley and Sons, 1986.
- [6] Book, W. J., "Recursive Lagrangian dynamics of flexible manipulator arms," *Int. J. of Robotics Research*, Vol.3, No.3, 1984, pp.87-101.
- [7] Yuan, B., "Adaptive strategies for controls of flexible arms," Ph.D. Thesis, Dept. of Mech. Engr., Ga. Tech., April 1989.
- [8] Leitmann, G., "On the efficacy of nonlinear control in uncertain linear systems," *ASME J. of Dynamic Systems, Measurement and Control*, 1981, PP.95.
- [9] Yuan, B., Book, W. J., Siciliano, B., "Direct adaptive control of a one-link flexible arm with tracking," Accepted to be published in *J. of Robotic Systems*.
- [10] Landau, Y. D., *Adaptive Control - the Model Reference Approach*, Marcel Dekker Inc., 1979.
- [11] Yuan, B. S., Book, W. J., Huggins, J. D., "Small motion experiments on large flexible arm with strain feedback," *1989 American Control Conference*, June 1989.

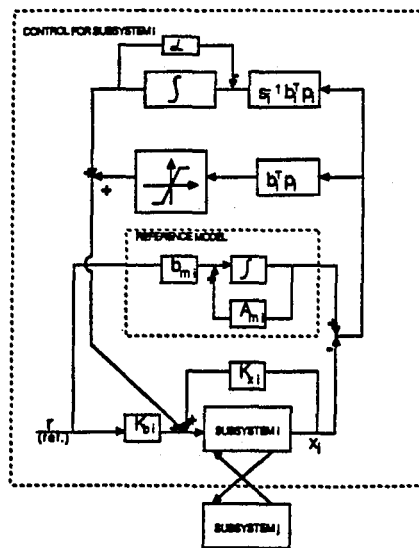


Figure 1. Block Diagram of the Decentralized Adaptive Control.

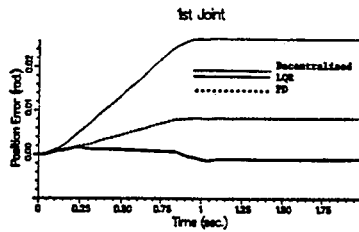


Figure 2a. Error Response of 1st Joint (Without Payload).

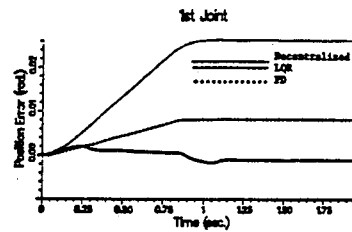


Figure 3a. Error Responses of 2nd Joint (With Payload).

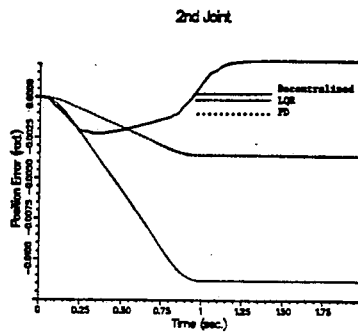


Figure 2b. Error Responses of 2nd Joint (Without Payload).

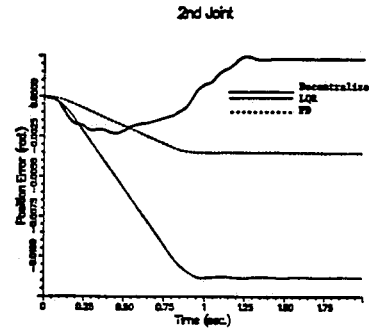


Figure 3b. Error Responses of 2nd Joint (With Payload).

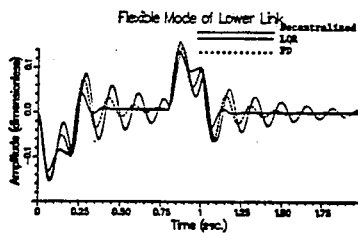


Figure 2c. Strain Responses of Lower Link (Without Payload).

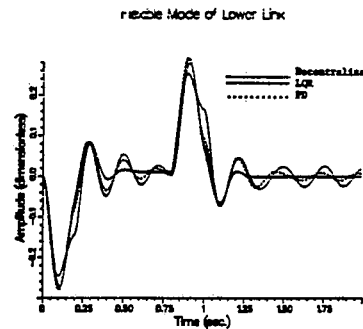


Figure 3c. Strain Responses of Lower Link (With Payload).

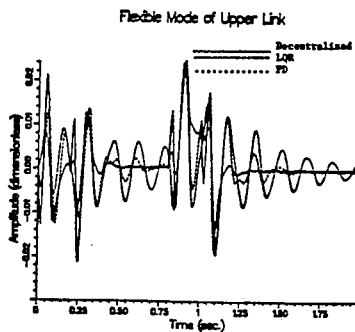


Figure 2d. Strain Responses of Upper Link (Without Payload).

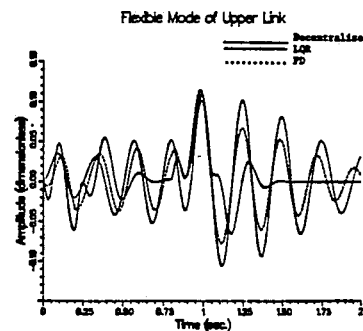


Figure 3d. Strain Responses of Upper Link (With Payload).

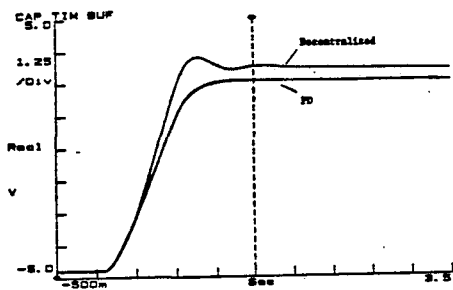


Figure 4a. Time Responses of 1st LVDT (Without Payload).

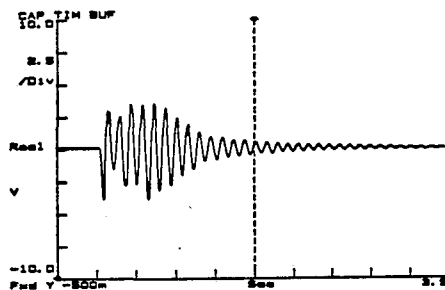


Figure 4e. Strain Response of Upper Link (PD, Without Payload).

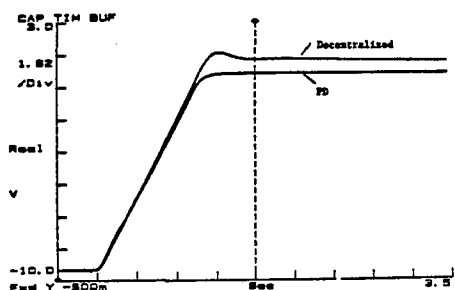


Figure 4b. Time Responses of 2nd LVDT (Without Payload).

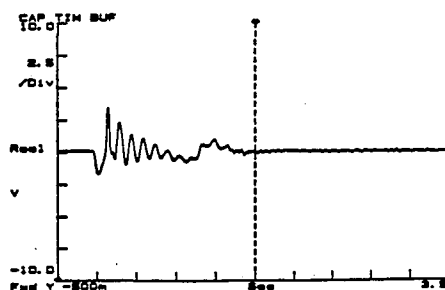


Figure 4f. Strain Response of Upper Link (Decentralized, Without Payload).

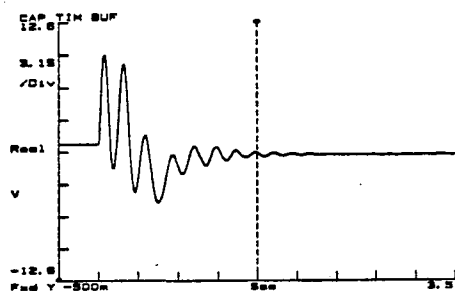


Figure 4c. Strain Responses of Lower Link (PD, Without Payload).

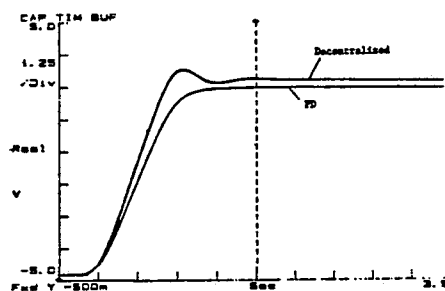


Figure 5a. Time Responses of 1st LVDT (With Payload).

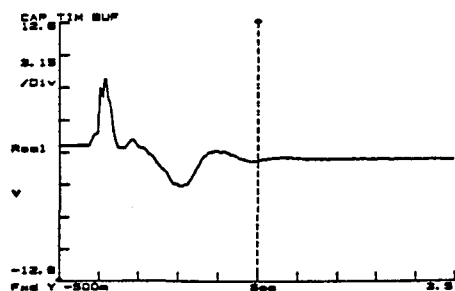


Figure 4d. Strain Response of Lower Link (Decentralized, Without Payload).

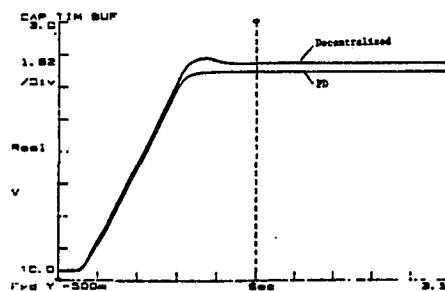


Figure 5b. Time Response of 2nd LVDT (With Payload).

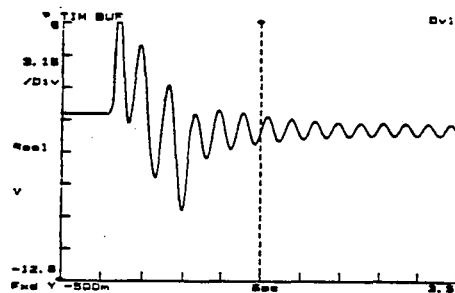


Figure 5c. Strain Response of Lower Link (PD, With Payload).

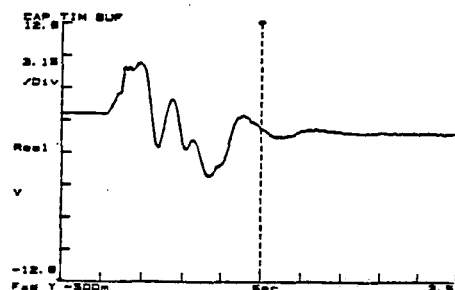


Figure 5d. Strain Response of Lower Link (Decentralized, With Payload).

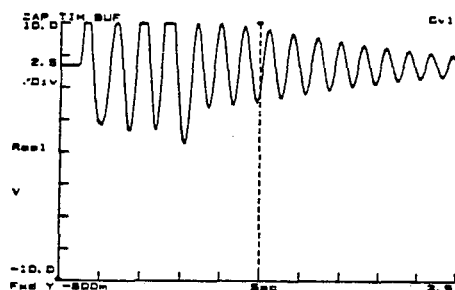


Figure 5e. Strain Response of Upper Link (PD, With Payload).

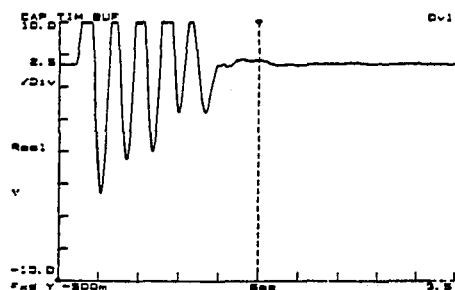


Figure 5f. Strain Response of Upper Link (Decentralized, With Payload).